

Synthesis of Brillouin frequency shift profiles to compensate non-local effects and Brillouin induced noise in BOTDA sensors

Javier Urricelqui, Mikel Sagues, and Alayn Loayssa*

Departamento de Ingeniería Eléctrica y Electrónica, Universidad Pública de Navarra, Campus Arrosadia s/n, 31006 Pamplona, Spain

**alayn.loayssa@unavarra.es*

Abstract: We present a novel technique for Brillouin optical time domain analysis (BOTDA) sensors that simultaneously compensates non-local effects and reduces Brillouin noise. The technique relies on the wavelength modulation of the optical source to modify the Brillouin interaction between probe and pump waves during their propagation. The resulting Brillouin distribution mimics the wavelength modulation, creating a virtual Brillouin frequency shift profile along the sensing fiber. The fundamentals of the technique are first described theoretically and using numerical simulations. Then, proof-of-concept experiments demonstrate the capabilities of the system to reduce large variations of the pump power resulting from the interaction with high probe powers and to decrease the Brillouin induced noise enhancing the signal to noise ratio (SNR) of the system. Furthermore, we show, for the first time to our knowledge, measurements of the Brillouin distribution using an injected optical power higher than the Brillouin threshold of the fiber.

©2014 Optical Society of America

OCIS codes: (290.5900) Scattering, stimulated Brillouin; (060.2370) Fiber optics sensors; (999.999) Brillouin optical time domain analysis.

References and links

1. L. Thévenaz, S. F. Mafang, and J. Lin, "Effect of pulse depletion in a Brillouin optical time-domain analysis system," *Opt. Express* **21**(12), 14017–14035 (2013).
 2. R. Bernini, A. Minardo, and L. Zeni, "Long-range distributed Brillouin fiber sensors by use of an unbalanced double sideband probe," *Opt. Express* **19**(24), 23845–23856 (2011).
 3. J. Urricelqui, M. Sagues, and A. Loayssa, "BOTDA measurements tolerant to non-local effects by using a phase-modulated probe wave and RF demodulation," *Opt. Express* **21**(14), 17186–17194 (2013).
 4. A. David and M. Horowitz, "Low-frequency transmitted intensity noise induced by stimulated Brillouin scattering in optical fibers," *Opt. Express* **19**(12), 11792–11803 (2011).
 5. T. Shimizu, K. Nakajima, K. Shiraki, K. Ieda, and I. Sankawa, "Evaluation methods and requirements for the stimulated Brillouin scattering threshold in a single-mode fiber," *Opt. Fiber Technol.* **14**(1), 10–15 (2008).
 6. H. Shalom, A. Zadok, M. Tur, P. J. Legg, W. D. Cornwell, and I. Andonovic, "On the various time constants of wavelength changes of a DFB laser under direct modulation," *IEEE J. Quantum Electron.* **34**(10), 1816–1822 (1998).
 7. Y. Dong, L. Chen, and X. Bao, "Extending the sensing range of Brillouin optical time-domain analysis combining frequency-division multiplexing and in-line EDFAs," *J. Lightwave Technol.* **30**(8), 1161–1167 (2012).
 8. X. Bao, J. Dhlwayo, N. Heron, D. J. Webb, and D. A. Jackson, "Experimental and theoretical studies on a distributed temperature sensor based on Brillouin scattering," *J. Lightwave Technol.* **13**(7), 1340–1348 (1995).
 9. A. Zornoza, M. Sagues, and A. Loayssa, "Self-heterodyne detection for SNR improvement and distributed phase-shift measurements in BOTDA," *J. Lightwave Technol.* **30**(8), 1066–1072 (2012).
 10. K. Shiraki, M. Ohashi, and M. Tateda, "SBS threshold of a fiber with a Brillouin frequency shift distribution," *J. Lightwave Technol.* **14**(1), 50–57 (1996).
 11. L. Chen and X. Bao, "Analytical and numerical solutions for steady state stimulated Brillouin scattering in a single-mode fiber," *Opt. Commun.* **152**(1–3), 65–70 (1998).
 12. P. Bayvel and P. M. Radmore, "Solutions of the SBS equations in single mode optical fibres and implications for fibre transmission systems," *Electron. Lett.* **26**(7), 434–436 (1990).
-

1. Introduction

In the past few decades, Brillouin fiber sensors have attracted great interest in both academic and industrial sectors. In particular, Brillouin optical time domain analysis (BOTDA) sensors have been thoroughly studied in order to improve their performance. This attention is due to their capability to perform distributed measurements of temperature and strain with high spatial resolution over extremely large structures.

However, several effects constrain the ultimate distance range of BOTDA sensors. One of the main limitations comes from non-local effects, which restrict the maximum power of the probe wave and hence, the received signal to noise ratio (SNR). This detrimental effect is caused by the energy continuously transferred between the probe and pump waves along the fiber, which modifies the pump power by introducing a wavelength dependence that leads to errors in the Brillouin frequency shift (BFS) measurements [1]. Different works have focused on reducing this limitation by using special configurations of the BOTDA sensor, such as the use of a double probe wave [1,2] or our proposal for using an RF phase-modulated probe wave [3].

Another factor that limits the injection of high probe power into the fiber is noise initiated from spontaneous Brillouin scattering (SpBS), which leads to depletion of the launched signal and degradation of the SNR in the detected signal [4, 5]. This is another manifestation of the so-called Brillouin threshold of a fiber link [5].

In this paper, we present a new tool capable of increasing the monitoring distance achieved by BOTDA sensors. The technique is based on modulating the wavelength of the optical source in order to synthesize a virtual BFS along the fiber. We demonstrate, theoretically and experimentally, the potential of the virtual BFS technique to compensate non-local effects and reduce Brillouin induced noise.

2. Fundamentals

The principle of the proposed technique is schematically depicted in Fig. 1.

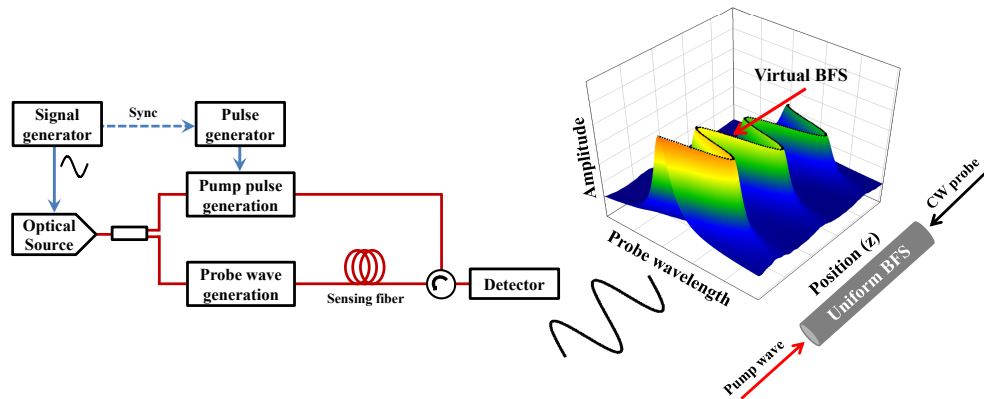


Fig. 1. Fundamentals of the laser wavelength dithering technique for virtual BFS synthesis.

This figure describes a conventional BOTDA setup based on a single source, although the technique is also applicable to double-laser setups. The laser source is divided in two branches. As it is well-known, a basic BOTDA setup requires the generation of a pump pulse and a CW probe that have a controlled wavelength difference, which should be tunable around the Brillouin frequency shift (BFS) of the deployed fiber. In Fig. 1, the upper branch is used to generate the pump pulses by pulsing the laser source signal and the lower branch is used to generate the probe wave. Depending on the particular type of BOTDA setup deployed, the frequency translation of the laser source signal required to have the tunable wavelength difference between pump and probe that is needed for Brillouin interaction may be performed either in the upper or lower branch, typically by the sideband generation

technique, i.e. using modulation in the microwave range to generate sidebands of the narrow laser source.

The only difference to a conventional BOTDA resides on the addition of a wavelength modulation of the optical source using a low frequency periodic wave that is synchronized to the pulse generator. This is performed using a small current modulation that modifies the instantaneous optical frequency of the optical source through the semiconductor laser's chirp (mostly adiabatic or thermal, depending on the modulation frequency [6]). Furthermore, the wavelength modulation shape is directly translated to a synthesized virtual BFS profile along the fiber as it is explained below. A sinusoidal wave is depicted in the figure as an example, but any other modulation shapes are possible.

In the upper branch, a synchronism signal activates the temporal switching of the modulated optical wave providing a pump pulsed signal, whose wavelength depends on the fixed propagation delay between the optical source and the optical switch. Then, this pump pulse is directed into the sensing fiber to interact with the probe wave via stimulated Brillouin scattering (SBS). However, in contrast to conventional BOTDA sensors, the wavelength of the probe wave varies along the optical fiber according to the wavelength modulation applied to the optical source. As a consequence, the pump pulse meets a probe wave of different wavelength at each location of the fiber. The resulting Brillouin interaction between both waves will be given by the detuning from the center of the Brillouin spectrum at each position of the fiber:

$$\Delta\nu(z) = \nu_p - \nu_s(z) - \text{BFS}(z) \quad (1)$$

where ν_p is the pump pulse wavelength and ν_s is the probe wave wavelength at position z . Note that the last expression points out that it is equivalent to have an actual variation in BFS due to the fiber characteristics than to have that same variation in ν_s . Therefore, a virtual BFS profile is synthesized by the probe wavelength modulation.

This synthesized virtual BFS profile can be used, for instance, to compensate non-local effects. The presented technique relies on the same idea that methods that use a sensing fiber made of fiber segments with different characteristic BFS [7]. The advantage is that there is no need to modify the fiber type along the sensing route, which is a cumbersome process. By using source wavelength modulation we are creating a virtual BFS profile along the sensing fiber.

Non-local effects are caused by the energy transfer between the probe wave and the pump pulse along its propagation. As a consequence, the pump power varies considerably due to its continuous interaction with the probe wave at each location of the fiber. Moreover, this variation of the pump power changes with the frequency difference between probe and pump waves. Therefore, the pump power acquires a wavelength dependence that distorts the measured Brillouin spectra and impairs the BFS measurement. The worst-case scenario occurs when the sensing fiber has a uniform BFS. In this case, the pump pulse experiences an identical Brillouin interaction during its propagation. This interaction changes for each pump pulse used to recover the BFS distribution. As a consequence, the wavelength dependence of the pump power acquires a Lorentzian shape, whose peak matches the BFS of the fiber [1]. However, using our technique we can ameliorate this problem because, even in the worst-case scenario, the wavelength difference of pump and probe waves varies along the sensing fiber, effectively synthesizing a virtual BFS. As a consequence of this position dependency, the energy transfer principally occurs at those locations where $\Delta\nu = 0$, i.e. where the difference between probe and pump wavelengths coincides with the natural BFS of the fiber. Therefore, there is less wavelength dependence of the pulse power and hence, less non-local effects and measurement error.

In order to theoretically study the compensation of non-local effects using the virtual BFS synthesis, we performed numerical simulations of the depletion factor of the pump power for the worst-case scenario (uniform BFS) and for different virtual BFSs. This factor is defined as [1]:

$$d = |P_p - P_{p0}| / P_{p0} \quad (2)$$

where P_p and P_{p0} are the pump powers with and without Brillouin interaction, respectively. Note that the last expression is equally defined for gain or loss based BOTDA configurations, even though the pump pulses are amplified using the latter one. However, both systems lead to an equally distorted Brillouin spectrum [1]. The pump power under Brillouin interaction can be simply calculated from the basic model that governs Brillouin interaction [8] yielding:

$$P_p(z) = P_p(0) \exp \left(\frac{-P_s(L) \exp(-\alpha L)}{A_{eff}} \int_0^z \frac{g_0}{1 + [2\Delta\nu(z)/\Delta\nu_B]^2} \exp(\alpha z) dz - \alpha z \right) \quad (3)$$

where $P_s(z)$ is the probe power at location z , A_{eff} is the effective area of the fiber, L is the fiber length, α is the attenuation of the optical fiber, g_0 is the local gain and $\Delta\nu_B$ is the Brillouin linewidth.

Figure 2(a) depicts the depletion factor of the pump power for the different simulated scenarios of synthesized BFS and uniform BFS represented in Fig. 2(b).

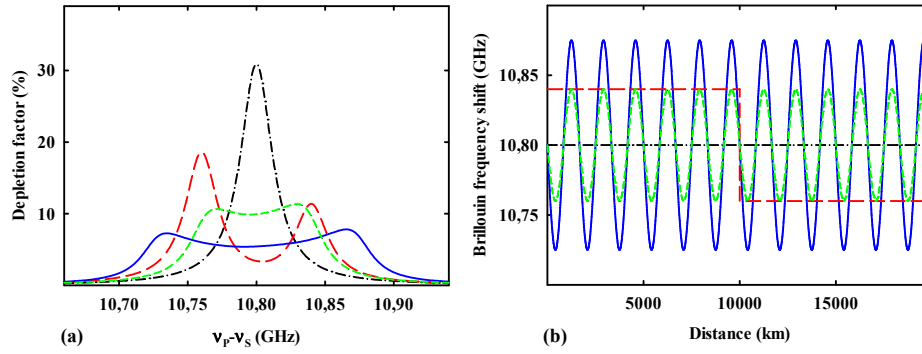


Fig. 2. (a) Calculated depletion factor of pump power using (b) different BFS distributions: a uniform BFS fiber (black-dot-dashed line), a virtual BFS based on two fiber segments (red-long-dashed line) and two sinusoidal virtual BFSs with a frequency modulation of 80 MHz (green-short-dashed line) and 150 MHz (blue-solid line) with 12 cycles along the fiber. Simulation's parameters are: $g_0 = 1.1 \cdot 10^{-11} \text{ m/W}$, $\Delta\nu_B = 30 \text{ MHz}$, $L = 20 \text{ km}$, effective area is $8 \cdot 10^{-11} \text{ m}^2$ and the injected optical pump and probe powers are 100 mW and 150 μW , respectively.

As it is shown, if the sensing fiber has a uniform BFS (10.8 GHz), the wavelength dependence of pump power shows a Lorentzian profile, whose peak matches the BFS. Note that for this pump power profile, the maximum depletion factor tolerated for a 1-MHz in BFS accuracy is 17% [1]. In this case, this value reaches a 30% change and the maximum error induced in the BFS measurement is around 2 MHz. This depletion of the pump power can be reduced by synthesizing a virtual BFS. For instance, using a square wave, we could simulate a sensing fiber with two equally-long segments, but different BFS values as shown in Fig. 2(b). Therefore, the energy transfer to the pump wave takes place at two frequencies instead of one, reducing the depletion. Note in Fig. 2(a) that a higher depletion takes place at the synthesized BFS that is located closer to the probe wave input as the Brillouin interaction is larger at that location. Another possibility is to synthesize a wavelength modulation that varies continuously along the fiber, for example, a sinusoidal virtual BFS, which spreads the energy transfer into a larger frequency range than the square modulation. As it is shown in Fig. 2(b), we have simulated two sinusoidal virtual BFSs with different frequency range. The one with lower modulation index clearly reduces the depletion as the Brillouin energy transfer has been spread into an 80-MHz frequency range, as it is shown in Fig. 2(a). In this case, the depletion factor has been reduced from 18% to 12% comparing to the square modulation, but it is still appreciable that one of the peaks is slightly higher than the other. This asymmetry is again

due to the distribution of the probe power, which is larger at the semi-cycle of BFS variation that coincides with the last kilometer of the sensing fiber. The last scenario presented in Fig. 2(a) is the sinusoidal virtual BFS with higher modulation index, which gets better results, bringing the depletion factor below 10% and ensuring a good performance in the BOTDA sensor. This result is due to the spreading of the interaction into a larger frequency range (150 MHz).

Note that the scenarios mentioned above are only examples that reveal the working principle of the technique and any other virtual BFS profiles can be implemented to reduce even more this detrimental effect. Finally, it must be mentioned that the presented technique could be combined with others schemes that reduce non-local effects to enhance even more the system's performance.

Another advantage of using this technique is the reduction of the Brillouin induced noise in the detected signal. This effect arises from the injection of high power components into the optical fiber, which can pump SBS amplification of thermally induced SpBS waves, in a process that leads to the onset of the so-called Brillouin threshold. This threshold establishes a maximum power that can be injected in a fiber before significant power begins to be reflected back and the launched signal is depleted. Moreover, it has been found that noise is added to the signal as it approaches the Brillouin threshold power [5]. This is an important problem for all types of BOTDA sensors, but particularly for those that deploy a modulated probe wave that tends to have a strong carrier [9]. In these setups, the Brillouin noise induced into the optical carrier is transferred to the detected RF signal when the injected carrier power approaches the Brillouin threshold, compromising its SNR performance.

The Brillouin threshold can be increased and the Brillouin induced detection noise reduced by implementing the virtual BFS technique. Again, the idea is to mimic those approaches that seek to increase the SBS threshold by using fiber links with a variation of BFS along their length [10], but synthesizing a virtual SBS profile instead of implementing a real one. We have numerically studied the Brillouin threshold increment when a virtual BFS is synthesized. This was accomplished by solving the numerical model based on the coupled intensity equations presented in [11]. This simulates that the thermally induced SpBS waves can be interpreted as a low power component injected at one end of the fiber. Figure 3 shows the backscattered and transmitted power resulting from gradually increasing the launched optical power for the worst-case scenario (a uniform BFS) and for a sinusoidal virtual BFS. Note that using the proposed technique, the Brillouin threshold rapidly increases from ~ 7 mW to ~ 44 mW (defined as the launched power at which the reflected power becomes 1% of the input power [12]). As a consequence, higher power can be injected into the fiber, enhancing the SNR value in detection.

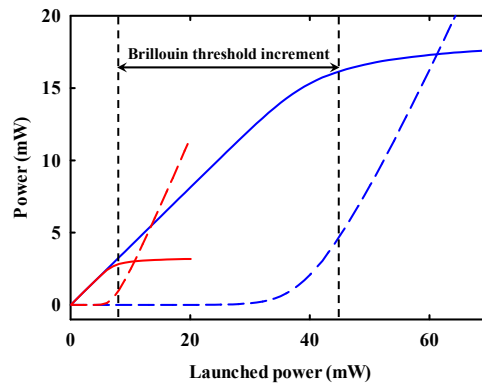


Fig. 3. Calculated reflected (dashed-line) and transmitted (solid-line) power using a uniform BFS fiber (red line) and a sinusoidal virtual BFS of 150 MHz frequency modulation and 12 cycles (blue line). Simulation parameters are: $g_0 = 1.1 \cdot 10^{-11}$ m/W, $\Delta\nu_B = 30$ MHz, $L = 20$ km, effective area is $8 \cdot 10^{-11}$ m² and the optical power injected to simulate SpBS waves is 7 nW.

3. Experimental setup and measurements

The BOTDA configuration used to demonstrate the potential of the technique is based on a phase modulated probe wave and RF demodulation [3]. This setup was chosen to simultaneously show the compensation of non-local effects and the reduction of Brillouin induced noise generated by the injection of a high optical carrier power. Figure 4 sketches the deployed experimental setup. As it was indicated before, the setup is modified to add a function generator, which is synchronized to the pulse generator, to directly modulate a 1560 nm high power DFB laser. The light from this modulated wavelength laser is coupled into two optical branches. In the upper branch, a double sideband suppressed carrier modulation is deployed with a Mach Zehnder electro-optic modulator (MZ-EOM) and then is pulsed using a semiconductor optical amplifier (SOA). The temporal switching provides a pulsed signal with a wavelength given by the time delay between the DFB and the SOA switch. This signal is amplified by an erbium-doped fiber amplifier (EDFA) and the upper-sideband of the pulsed signal is filtered by a narrowband fiber Bragg grating (FBG). Then, a polarization scrambler (PS) is used to reduce polarization induced fluctuations in the signal before launching the pulses into the sensing fiber via a circulator. In the lower branch, a probe wave is generated with an electro-optic phase modulator driven by a 1.3 GHz RF signal. Once the probe wave has interacted with the pump pulse via SBS, it is photodetected and the resultant RF signal is demodulated and captured in a digital oscilloscope. A 20-km standard single-mode fiber was deployed as sensing fiber.

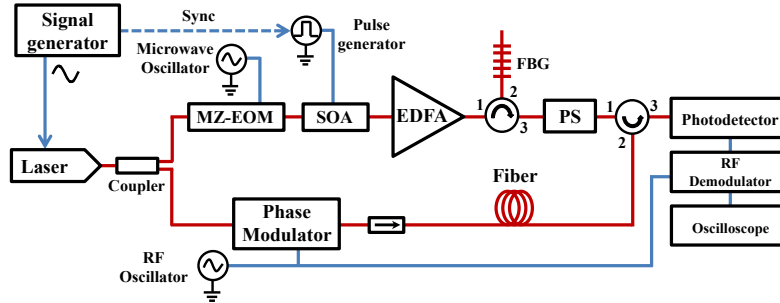


Fig. 4. Experimental setup for the BOTDA sensor based on virtual BFS synthesis technique.

Figure 5 compares the distribution of the measured Brillouin spectra along the fiber after and before applying the wavelength modulation to the optical source. In the former case, the output of the signal generator was chosen to be a sinusoidal signal of frequency 60 KHz and amplitude of 200 mV, which yields a wavelength modulated probe wave of 6 cycles for the 20-km long fiber and a maximum 150-MHz frequency shift, respectively. Notice that with this modulation, a sinusoidal virtual BFS distribution that mimics the wavelength modulation is synthesized. Other spectral profiles could be easily implemented, for instance, a wavelength modulation using a square wave with 5 kHz frequency would lead to a BFS profile equivalent to that of two concatenated 10 km fiber segments with different characteristic BFS value. Furthermore, as the wavelength modulation of the probe wave is known, the technique also offers the possibility to recover the natural BFS profile of the fiber by simply using Eq. (1).

Notice that, during the interaction between both waves, the wavelength variation of the probe wave must be low enough to avoid a loss of the measurement contrast. This limit is linked to the wavelength modulation parameters and hence, they must be carefully selected. Note also that direct modulation of the laser generates a small sinusoidal variation of the amplitude of the measured Brillouin spectra along the fiber, which has no implications on the sensor performance.

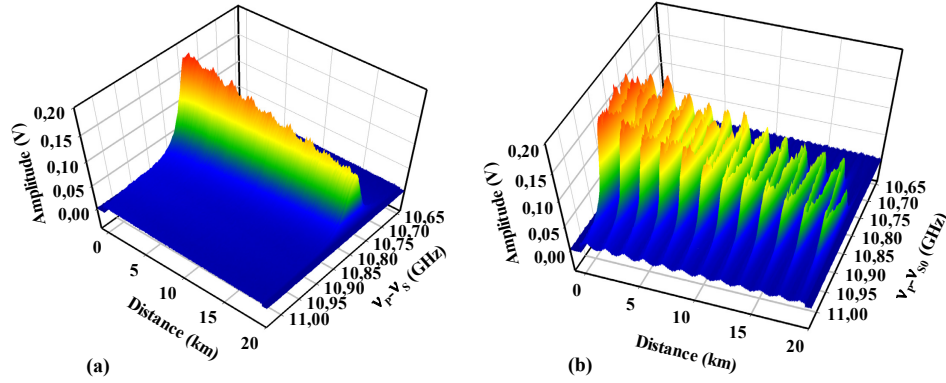


Fig. 5. (a) Experimental distribution of Brillouin spectra along the fiber for a conventional BOTDA measurement and (b) for a sinusoidal synthesized BFS distribution after applying modulation to the optical source (ν_{s0} is the optical carrier frequency, when no modulation is applied to the laser source).

In order to study the potential of the system regarding non-local effects, the probe power was set to a value high enough (0.34 mW) to induce a significant wavelength dependence on the pump power. The deployed BOTDA sensor was set in a loss-based configuration and hence, the pump pulses were amplified during their propagation. Figure 6(a) compares the amplification factor of the pump power using the conventional technique and after applying the wavelength modulation to the laser source. Notice that the technique brings the gain factor below the 17% required to ensure less than 1°C measurement error in the worst-case scenario, which is given by the deployment of a long optical fiber with a uniform BFS followed by a final section with a different BFS [1]. This scenario was simulated by inserting the last meters of the optical fiber into a climatic chamber at 50 °C. Figure 6(b) shows the measured Brillouin spectra at the heated section before and after synthesizing a virtual BFS. Notice that the measured spectrum using the conventional technique is clearly distorted by the transfer function induced by the pump power wavelength dependence, which clearly biases its peak. On the other hand, the Brillouin spectrum is perfectly recovered using the virtual BFS technique, as expected, since the pump power does not present this wavelength dependence. Note that the frequency difference between the virtual BFS profile and the natural BFS profile of the fiber has been corrected in order to compare both spectra.

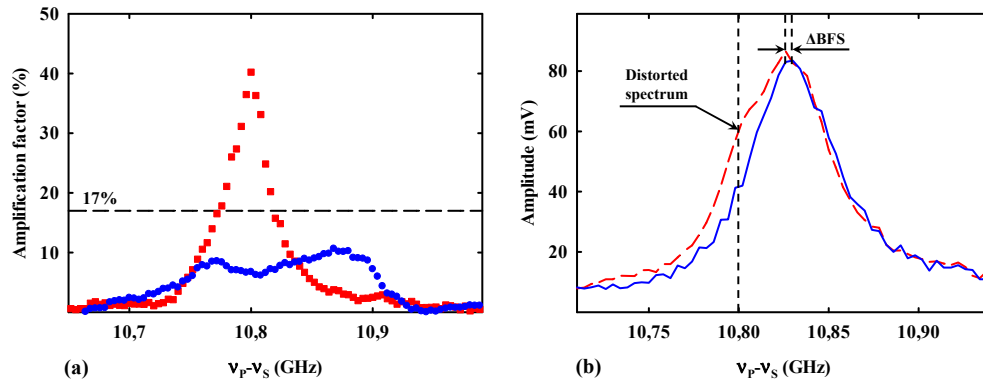


Fig. 6. (a) Measured gain factor of the pump power as a function of the frequency separation between pump and probe waves after (blue circles) and before (red squares) the source wavelength modulation is turned on. (b) Measured Brillouin spectra using the conventional technique (red-dashed line) and using the sinusoidal synthesized BFS distribution (blue-solid line).

Another set of experiments was performed to highlight the potential to reduce Brillouin induced noise and increase the Brillouin threshold. The power of the injected carrier was gradually increased without applying the wavelength modulation until the appearance of Brillouin noise at around 5 mW. Then, the carrier power was raised to 9 mW and Brillouin spectrum measurements were performed turning on and off the wavelength modulation (Fig. 7). As it is shown, the Brillouin noise induced in the RF signal leads to a noisy spectrum, while the presented technique greatly reduces the noise in the trace. The SNR enhancement between both measurements was quantified to be 10.17 dB, which was measured by computing the standard deviation of the detected noise.

Note that the measured Brillouin spectrum using the presented technique deploys an optical carrier power that outreaches the Brillouin threshold of the used sensing fiber, which was experimentally measured as 7.9 mW. We would also like to remark that the optical power injected into the fiber was limited by the available power and hence, a higher optical carrier power could be deployed to enhance even more the achieved SNR. Furthermore, the probe power was set to 0.236mW to also compensate non-local effects.

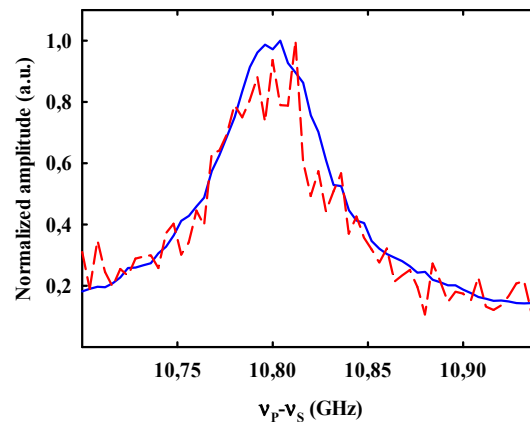


Fig. 7. Measured Brillouin spectra turning on (blue-solid line) and off (red-dashed line) the wavelength modulation applied to the laser source.

Finally, the BOTDA sensor with BFS synthesis was used for temperature measurements, obtaining for the particular experimental conditions used, 1-m resolution and around 1°C uncertainty at the end of the fiber (worst-case).

4. Conclusions

In this paper, we have presented a new concept for BOTDA sensors based on the synthesis of a virtual BFS profile along the sensing fiber. The technique relies on the wavelength modulation of an optical source using a periodic signal that is synchronized to the pulse generator. The technique has been theoretically studied and proof-of-concept experiments have been performed to demonstrate the generation of this virtual BFS profile and its application to solving two of the fundamental problems presented in long-range BOTDA sensors: non local effects and Brillouin induced noise. Further work should focus on studying the system's performance regarding the maximal probe power that can be injected into the fiber, the achievable sensing range or the most appropriate kind of wavelength modulation used to reduce non-local effects. This novel and simple tool is bound to find other interesting applications in Brillouin distributed sensing and signal processing.

Acknowledgments

The authors wish to acknowledge the financial support from the Spanish Ministerio de Ciencia e Innovación through the project TEC2010-20224-C02-01 and from the Universidad Pública de Navarra.